Weakly-nonlinear seakeeping model: regular/irregular wave interaction with a ship without/with forward speed

M. Greco[1,2] **B. Bouscasse**[1] **G. Colicchio**[1,2] **C. Lugni**[1,2]
m.greco@insean.it b.bouscasse@insean.it g.colicchio@insean.it c.lugni@insean.it

1 **INSEAN, Italian Ship Model Basin, Roma – Italy.**
2 **Centre for Ships and Ocean Structures (CeSOS), NTNU, Trondheim – Norway.**

Present investigation concerns the further development of the numerical potential-flow method described in Greco *et al*. (2008). This couples (A) a 3D weakly nonlinear solver based on the weak-scatterer hypothesis (Pawlowski 1991) with (B) a 2D shallow-water solver on the deck plane, which handle, respectively, the ship seakeeping and the water shipping.

The boundary conditions for the shallow-water problem have been improved when a bulwark is present, both in terms of the deck-plane velocity (u, v) and of the water level h: the partial reduction of the water flow through the local deck contour and the partial reflection of the liquid by the obstacle are accounted for. The former is introduced as a correction of the shallow-water velocity solution, the latter is enforced as a liquid layer to be added to the deck-contour water level given as boundary condition by the external field. The latter, *i.e.* the h boundary condition from the seakeeping problem is different than zero only during a water-on-deck phase. A simplified criterion for the slamming occurrence has been implemented, based on the impact angle and the pressure level associated with the phenomenon. The slamming and water-entry local loads were handled by means of a Wagner-theory approach (Wagner 1932). The solution method has been extended to handle the forward motion of the vessel, under the assumptions of small ship speed U_{ship} and following the work by Salvesen *et al*. (1970). It means that the forward-motion effects are introduced as an explicit correction of: (a) the zero-speed frequency-dependent hydrodynamic coefficients, (b) the Froude-Krylov load contribution and (c) the wave field around the vessel. This approximation has the advantage of being computationally cheap, but its applicability is limited and must be assessed. Finally, the solver description of the incoming waves has been extended to handle irregular waves as a superposition of linear regular waves. Regular-sea conditions are described instead as second-order Stokes' waves.

The resulting method was applied to investigate the seakeeping of a patrol ship without and with forward motion and interacting with regular and irregular incident waves. The results were compared against model tests already performed at INSEAN and newly carried out at the scale 1:20 (INSEAN C2364 model long $L = 4$ m). Here the head-sea conditions are discussed. In the experiments, to limit the oscillations along the longitudinal axis and make the video recording of the water-on-deck events easier, the self-propelled model was fixed to the carriage through a gimble. The vessel was then free to heave and pitch around the center of mass, while the remaining rigid motions have been prevented.

Ship interaction with regular incoming waves

Rigid motions, water-on-deck occurrence and added-wave resistance have been examined.

$Fr = 0$					$Fr = 0.189$				
kA λ/L	0.75	1.0	1.25	1.5	kA λ/L	0.75	1.0	1.25	1.5
0.1	NO/NO	NO/NO	NO/NO	NO/NO	0.1	NO/NO	NO/NO	YES/NO	YES/NO
0.25	NO/NO	YES/YES	YES/YES	YES/YES	0.15	NO/NO	YES/YES	YES/YES	YES/YES

Table 1: Regular waves: cases examined. $\lambda = 2\pi/k$ and A are the length and the amplitude of the incoming waves. Occurrence of water on deck is indicated through the boolean variables representing, in sequence, the experimental and numerical solution. $Fr = U_{ship}/\sqrt{(gL)}$, with U_{ship} and L the ship speed and length and g the gravity acceleration.

Motions The measured motions were compared with the corresponding curves predicted numerically by the weakly-nonlinear solver for several incoming-wave conditions. Table 1 summarizes the cases that will be examined. Globally the agreement is satisfactory both for heave and pitch (the comparison is not shown here but for the example in the later figure 2), though in some cases the numerical results underestimate the experimental data. In particular this is true at the lowest wavelength. Numerically the forward motion is responsible for larger pitch and heave. This is true also experimentally but for the shortest incident waves where the pitch reduces and the heave does not change much with the Froude number $Fr = U_{ship}/\sqrt{(gL)}$, U_{ship} being the ship speed. Such incoming-wave case is associated with quite limited amplitudes so it is more sensitive to the experimental set-up and to the numerical accuracy. Both experimentally and numerically a greater steepness kA tends to cause a smaller motion amplitude. This is especially true for the pitch motion while the behavior is more complex for the heave. Here, k and A are the wavenumber and wave amplitude, respectively.

Water-on-deck occurrence Table 1 is also explicative of the measured and predicted water shipping events for the selected incoming-wave cases. Experiments and numerics agree in terms of water-on-deck occurrence at $Fr = 0$ (see left of table 1). There is no water shipping for wavelength-to-ship length ratio $\lambda/L = 0.75$, while the longer waves examined are responsible for water on deck at the highest steepness. The shortest incident waves do not cause water shipping also at $Fr = 0.189$ (see right of table 1). The longer ones lead to water on deck both numerically and experimentally at

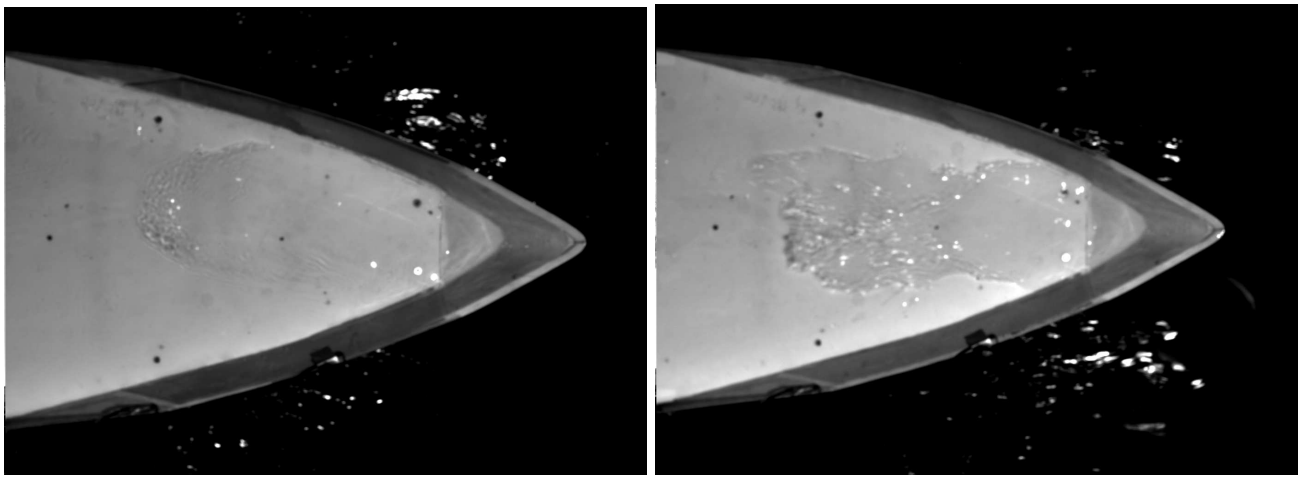

Figure 1: Regular waves. Water on deck events for $\lambda = 1.25L$ (left) and $\lambda = 1.5L$ (right), $kA = 0.1$ and $Fr = 0.189$. Top view from the experimental video recordings. In the plots the incoming waves propagate from right to left.

$kA = 0.15$, while at $kA = 0.1$ the water-shipping occurrence is recorded in the physical case only. However the video recording of the model tests highlight events very gentle and with a little amount of shipped water in these cases, as shown in figure 1. In the plots the incoming waves propagate from right to left. The snapshots refer to the later stages of a generic event for the two incoming-wave cases: the very short water-shipping phase is over and there is a rather limited amount of liquid onto the deck. One can expect that such water-on-deck phenomena are not relevant for the vessel. This is suggested

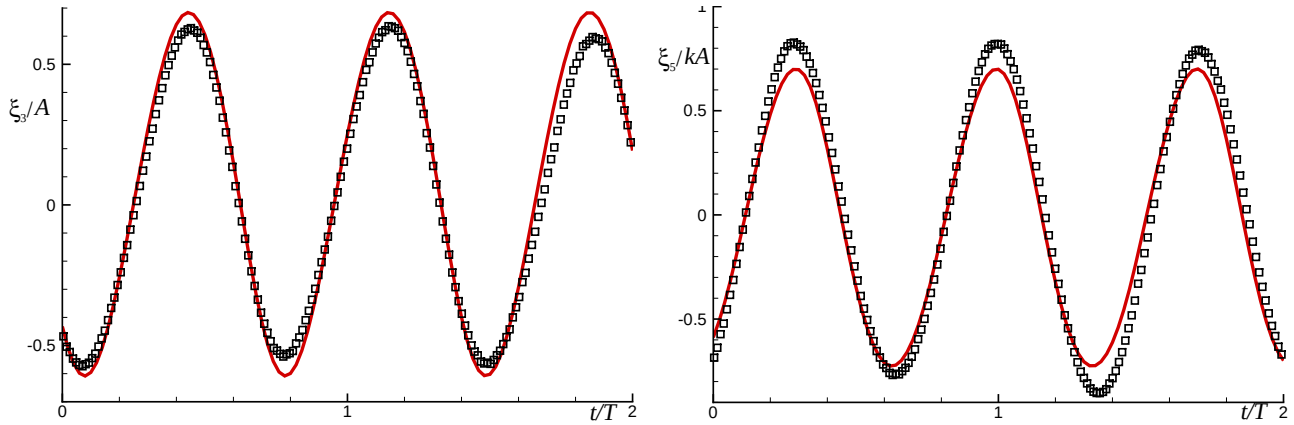

Figure 2: Regular waves. Heave (left) and pitch (right) time histories for $\lambda = 1.25L$, $kA = 0.1$ and $Fr = 0.189$. Empty squares: experiments; solid lines: weakly-nonlinear solution. T is the incoming-wave period.

by the fair agreement between the measured and predicted ship motions, shown in figure 2 for $\lambda/L = 1.25$. The reason why the numerical solver is not able to predict these water-shipping events can be partially found in the approximation of the wave-field description. In particular the swell-up associated with the forward motion is disregarded. Also trim and sinkage were not accounted for but this error source should not be relevant because they appeared limited in the model tests.

Added-wave resistance The nonlinear ship interaction with incoming waves is responsible for a mean non-zero value of the longitudinal force acting on the vessel. This added-wave resistance, R_{aw}, represents in its nature a second-order effect and is examined in figure 3 for the cases in table 1. The results highlight a reasonable agreement between the experiments and the numerical solution. This is quite promising if one considers the different approaches used to estimate this force numerically and experimentally. In the simulations, R_{aw} was calculated in the reference frame moving with the ship forward speed as the mean force acting in the longitudinal ship axis x and obtained by direct pressure integration. In the experiments, the added resistance in waves was measured as the averaged force along x given by the load cell on the

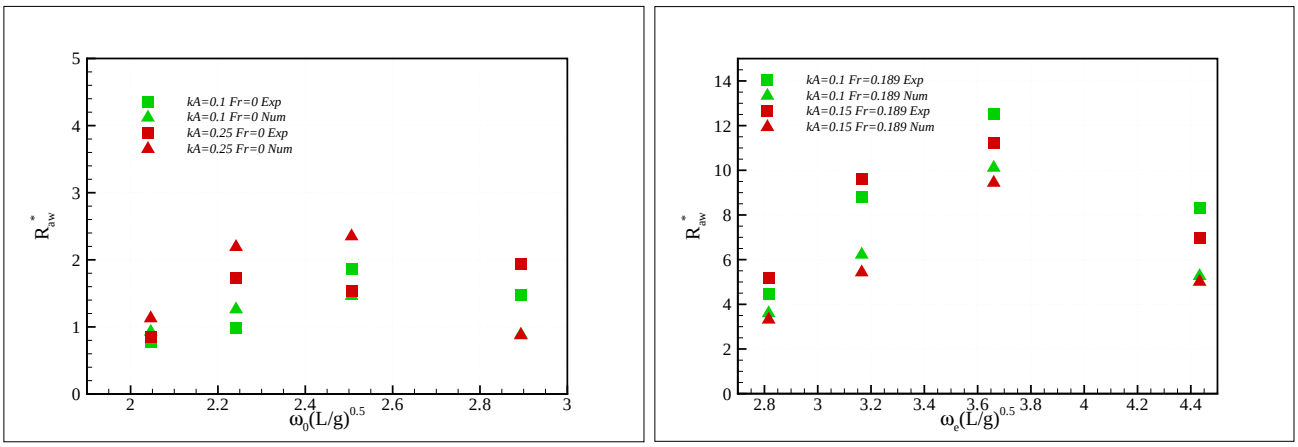

Figure 3: Regular waves. Added-wave resistance R_{aw} versus the incoming wave frequency ω_0 (left) and encounter frequency ω_e (right), as measured at model scale and predicted numerically. Left plot: $Fr = 0$. Right plot: $Fr = 0.189$. R_{aw} is made nondimensional by $1/2\rho g(A^2B^2/L)$. Here g is the gravity acceleration, A is the incoming-wave amplitude, and B and L are the breadth and length of the ship.

gimble. This was possible because the used propeller rps corresponds to the model propulsion point. The prediction tool and the model tests furnish globally a consistent trend of R_{aw} as a function of the incoming-wave frequency and steepness. R_{aw} reaches the highest values within an intermediate interval of the incoming-wave frequency ω_0 (or encounter frequency ω_e) and tends to be limited otherwise. At zero forward motion, in most of the cases R_{aw} increases with kA. Its behavior is more complex with the steepness at $Fr = 0.189$.

Ship interaction with irregular incident waves

Different irregular incident waves have been examined, here the ship interaction with the sea state in the top-left plot of figure 4 is discussed. The Response Amplitude Operators (RAOs) for the heave and pitch motions measured on the C2364 model at $Fr = 0$ and $Fr = 0.189$ are given in the top-right and bottom-left plots of figure 4. The experimental data are compared with the weakly-nonlinear and linear solutions. From the results, higher Fr causes a larger RAO within the examined range of λ/L. Roughly the response has a nearly linear behavior. Nonlinear effects play a role for wavelengths comparable or larger than the ship length. They lead to a heave response lower than the one predicted by the linear model, while the pitch response presents more complex features. Globally the weakly-nonlinear model recovers the linear behavior when the nonlinear effects are negligible and improves the linear solution otherwise. The last plot of figure 4 refers to a higher Froude number, *i.e.* $Fr = 0.275$. For this case full-scale measurements are available, also reported in the figure. More in detail, the almost uni-directional full-scale spectrum was measured through a wave radar system and its primary direction (reported in the top-left plot of figure 4) was reproduced in the INSEAN wave basin and in the numerical simulations. The full-scale data appear slightly more linear than those recorded at model scale, and agree quite well with the numerical solutions. This assesses the applicability of the simplified formulation used to handle the forward motion at least up to this Froude number. For a proper comparison an experimental uncertainty analysis should be performed, both at model and at full scale. Moreover a time-independent statistical study should be assessed both from numerical and experimental point of view. In the present case the results were obtained recording and simulating the ship-wave interaction for a duration equivalent to 30 min at full scale.

The extensions of the solver and the detailed results of the investigation will be discussed at the Workshop. This includes also water-on-deck and slamming occurrence in more severe irregular sea conditions.

This research activity is partially supported by the Centre for Ships and Ocean Structures (CeSOS), NTNU, Trondheim, within the ”Violent Water-Vessel Interactions and Related Structural Loads” project, partially supported by the Italian Navy within the ”6-dof RANSE” project and partially done within the framework of the ”Programma di Ricerca sulla Sicurezza” funded by *Ministero Infrastrutture e Trasporti*.

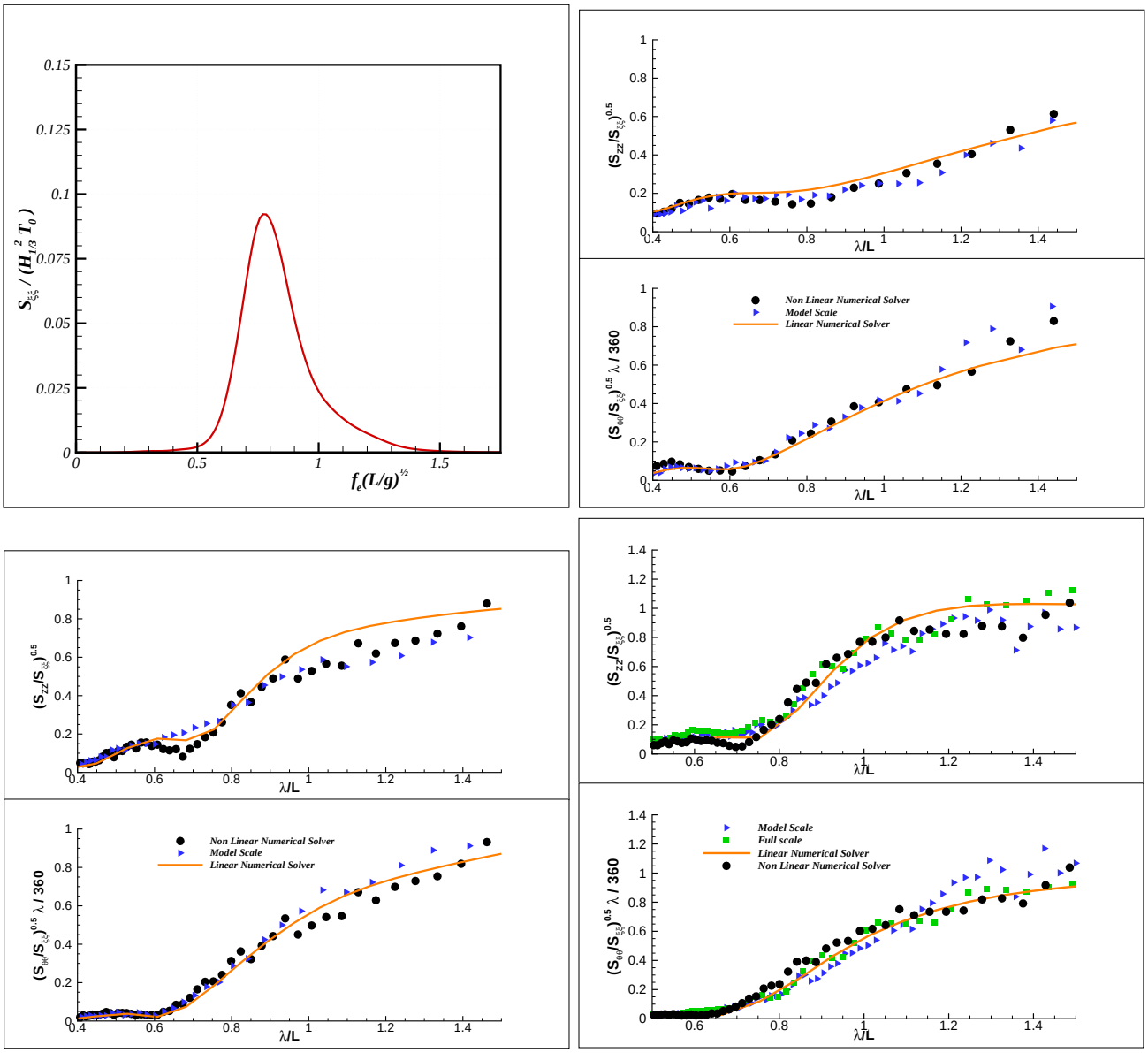

Figure 4: Irregular waves. Top left: spectrum of the studied sea state. $H_{1/3}$ and T_0 are are the significant wave height and the modal period, respectively. f_e is the encounter frequency (in Hz). Remaining plots: Response Amplitude Operator (RAO) for heave (top of each plot) and pitch (bottom of each plot) as measured at model scale, and predicted by linear and weakly-nonlinear models at $Fr = 0$ (top right), $Fr = 0.189$ (bottom left) and $Fr = 0.275$ (bottom right). For the highest forward speed also full-scale data are given.

References

GRECO, M., T. BAZZI, G. COLICCHIO, AND C. LUGNI (2008). 3D ship-seakeeping problem : weak-scatterer theory plus shallow-water on deck. In 23^{rd} *Int. Workshop of Water Waves and Floating Bodies*, Jeju, Korea.

PAWLOWSKI, J. (1991). A theoretical and numerical model of ship motions in heavy seas. In *SNAME Transactions*, Volume 99, pp. 319–315.

SALVESEN, N., E. O. TUCK, AND O. M. FALTINSEN (1970). Ship motions and sea loads. *Trans. SNAME 78*, 250–287.

WAGNER, H. (1932). Uber stoss- und gleitvorgange an der oberflache von flussigkeiten. *ZAMM 12*(4), 192–235.